Synthesis and Structure of the Tantalum Trimethyl Complex $[P_2N_2]TaMe_3$ and Its Conversion to the Tantalum Methylidene Species $[P_2N_2]Ta{=}CH_2(Me)$ ($[P_2N_2]$ = $PhP(CH_2SiMe_2NSiMe_2CH_2)_2PPh$)

Michael D. Fryzuk,* Samuel A. Johnson, and Steven J. Rettig†

Department of Chemistry, University of British Columbia, 2036 Main Mall, Vancouver, British Columbia, Canada V6T 1Z1

Received April 9, 1999

A tantalum(V) trimethyl complex and its photolysis product, a relatively stable tantalum(V) methyl methylidene, were prepared using the macrocyclic bis(amido-phosphine) $PhP(CH_2SiMe_2NSiMe_2CH_2)_2PPh$, abbreviated $[P_2N_2]$, as an ancillary ligand. The methylidene precursor $[P_2N_2]TaMe_3$ is generated by the reaction of $[P_2N_2]Li_2{\cdot}C_4H_8O_2$ ($C_4H_8O_2$ = 1,4-dioxane) with $TaMe_3Cl_2$. The solid-state X-ray molecular structure demonstrates that the geometry of $[P_2N_2]TaMe_3$ is a seven-coordinate capped trigonal prism, and NMR studies confirm this is also true in solution at low temperature. Photolysis with a UV source generates $[P_2N_2]Ta{=}CH_2(Me)$, with the elimination of methane. The X-ray solid-state molecular structure of $[P_2N_2]Ta{=}CH_2(Me)$ is intermediate between octahedral and trigonal-prismatic geometry. Variable-temperature NMR studies demonstrate that the double-bonded methylidene moiety rotates with a barrier of 33.5 ± 0.6 kJ/mol, in contrast to the larger barrier estimated for the previously characterized 18-electron complex $(\eta^5\text{-}C_5H_5)_2Ta{=}CH_2(Me)$. Reaction of $[P_2N_2]TaMe_3$ with $Ph_3C^+BF_4^-$ or $PhNMe_2H^+B(C_6F_5)_4^-$ produced $\{[P_2N_2]TaMe_2\}^+\text{-}BF_4^-$ and $\{[P_2N_2]TaMe_2\}^+B(C_6F_5)_4^-$, respectively. Attempts to deprotonate $\{[P_2N_2]TaMe_2\}^+$ did not provide a chemical route to $[P_2N_2]Ta{=}CH_2(Me)$ and instead generated either $[P_2N_2]\text{-}TaMe_2F$ or the product of deprotonation of the $[P_2N_2]$ ligand methylene backbone, $Ta(Me_2)[(CHSiMe_2NSiMe_2CH_2P(Ph)CH_2SiMe_2NSiMe_2CH_2PPh)]$, depending on the base and counteranion used.

Introduction

The synthesis of $(\eta^5\text{-}C_5H_5)_2Ta{=}CH_2(Me)$, the first stable methylidene complex,[1−4] served as one of the starting points for the preparation of a new family of metal−carbon multiple bonds.[5] This compound has since found applications as a precursor to catalytically active early−late heterobimetallics,[6] as well as in the study of the Fischer−Tropsch process[7] and in methylidene-transfer processes.[8] While a number of other stable methylidene complexes have been prepared, most, like the aforementioned tantalum complex, are coordinatively saturated species,[9,10] and the majority involve the late transition metals.[11−18] Some recent group 5 examples are $[PhC(NSiMe_3)_2]_2Ta{=}CH_2(Me)$[19] and the thermally unstable derivative $(ArO)_2Ta{=}CH_2(Me)$.[20,21] We have recently reported the preparation of the new macrocyclic ligand $[P_2N_2]$ (where $[P_2N_2]$ = $PhP(CH_2\text{-}SiMe_2NSiMe_2CH_2)_2PPh$)[22] and have shown that it can stabilize high-oxidation-state derivatives that contain Zr(IV)[23] or Al(III)[24] as well as group 3 metal centers such

† Professional Officer: UBC X-ray Structural Laboratory (deceased October 27, 1998).

(1) Schrock, R. R. *J. Am. Chem. Soc.* **1975**, *97*, 6577−6578.
(2) Guggenberger, L. J.; Schrock, R. R. *J. Am. Chem. Soc.* **1975**, *97*, 6578−6579.
(3) Schrock, R. R.; Sharp, P. R. *J. Am. Chem. Soc.* **1978**, *100*, 2389.
(4) Takusagawa, F.; Koetzle, T. F.; Sharp, P. R.; Schrock, R. R. *Acta Crystallogr., Sect. C: Cryst. Struct. Commun.* **1988**, *C44*, 439−443.
(5) Schrock, R. R. *Acc. Chem. Res.* **1979**, *12*, 98.
(6) Hostetler, M. J.; Bergman, R. G. *J. Am. Chem. Soc.* **1990**, *112*, 8621−8623.
(7) Proulx, G.; Bergman, R. G. *Science* **1993**, *259*, 661−663.
(8) Berry, D. H.; Koloski, T. S.; Carroll, P. J. *Organometallics* **1990**, *9*, 2952−2962.
(9) Antonelli, D. M.; Schaefer, W. P.; Parkin, G.; Bercaw, J. E. *J. Organomet. Chem.* **1993**, *462*, 213−220.
(10) van Asselt, A.; Burger, B. J.; Gibson, V. C.; Bercaw, J. E. *J. Am. Chem. Soc.* **1986**, *108*, 5347−5349.
(11) Heinekey, D. M.; Radzewich, C. E. *Organometallics* **1998**, *17*, 51−58.
(12) Gunnoe, T. B.; White, P. S.; Templeton, J. L.; Casarrubios, L. *J. Am. Chem. Soc.* **1997**, *119*, 3171−3172.
(13) Schwab, P.; Grubbs, R. H.; Ziller, J. W. *J. Am. Chem. Soc.* **1996**, *118*, 100−110.
(14) Fryzuk, M. D.; Gao, X.; Joshi, K.; MacNeil, P. A.; Massey, R. L. *J. Am. Chem. Soc.* **1993**, *115*, 10581−10590.
(15) Burrell, A. K.; Clark, G. R.; Rickard, C. E. F.; Roper, W. R.; Wright, A. H. *J. Chem. Soc., Dalton Trans.* **1991**, 609−614.
(16) Roger, C.; Lapinte, C. *J. Chem. Soc. Chem. Commun.* **1989**, 1598−1600.
(17) Hill, A. F.; Roper, W. R.; Waters, J. M.; Wright, A. H. *J. Am. Chem. Soc.* **1983**, *105*, 5939−5940.
(18) Patton, A. T.; Strouse, C. E.; Knobler, C. B.; Gladysz, J. A. *J. Am. Chem. Soc.* **1983**, *105*, 5804−5811.
(19) Dawson, D. Y.; Arnold, J. *Organometallics* **1997**, *16*, 1111−1113.
(20) Chamberlain, L. R.; Rothwell, A. P.; Rothwell, I. P. *J. Am. Chem. Soc.* **1984**, *106*, 1847.
(21) Chamberlain, L. R.; Rothwell, I. P. *J. Chem. Soc., Dalton Trans.* **1987**, 163.
(22) Fryzuk, M. D.; Love, J. B.; Rettig, S. J. *J. Chem. Soc., Chem. Commun.* **1996**, 2783.
(23) Fryzuk, M. D.; Love, J. B.; Rettig, S. J. *Organometallics* **1998**, *17*, 846−853.
(24) Fryzuk, M. D.; Giesbrecht, G. R.; Rettig, S. J. *Inorg. Chem.* **1998**, *37*, 6928−6934.

10.1021/om990249t CCC: $15.00
Publication on Web 09/03/1999

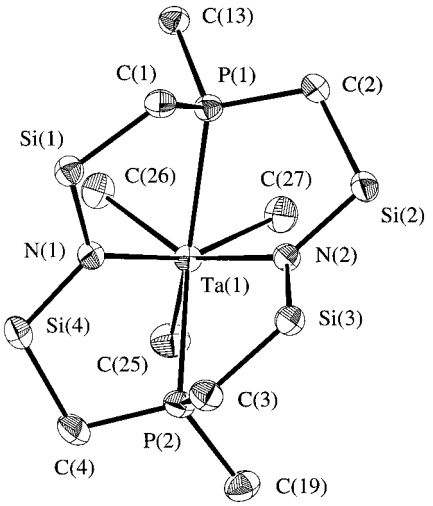

Figure 1. ORTEP representation of the solid-state molecular structure of $[P_2N_2]TaMe_3$ (**1**).

as Y(III).[25] In this paper we report the synthesis, structure, and fluxional behavior of methyl and methylidene complexes of Ta(V) stabilized by this macrocyclic ligand.

Results and Discussion

Synthesis and Structure of $[P_2N_2]TaMe_3$ (1). Attempts to isolate $[P_2N_2]TaCl_3$ from the reaction of $[P_2N_2]Li_2{\cdot}C_4H_8O_2$ ($C_4H_8O_2$ = 1,4-dioxane) and $TaCl_5$ have proven unsuccessful, despite several attempts under a variety of conditions. However, the reaction of the ligand precursor $[P_2N_2]Li_2{\cdot}C_4H_8O_2$ with the alternative starting material $TaMe_3Cl_2$[3,26] provides $[P_2N_2]$-$TaMe_3$, (**1**), in 80% yield (eq 1). Because the yellow

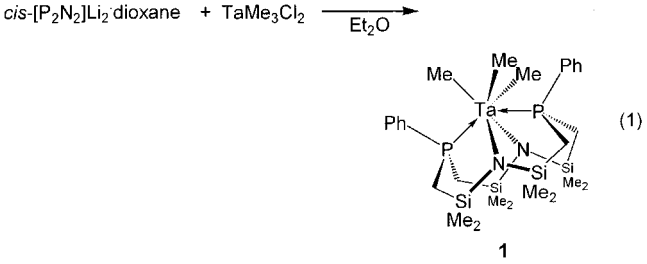

trimethyl species **1** is only moderately soluble in hexanes, it can be separated from the more soluble dark-colored impurities by rinsing the crude materials with hexanes.

The solid-state molecular structure is shown in Figure 1; crystals of **1** contain 0.5 equiv of cocrystallized hexanes per $[P_2N_2]TaMe_3$ molecule. Crystallographic data are given in Table 1. The complex can be regarded as a capped trigonal prism, where P(1) caps a rectangular face of the prism defined by C(26), C(27), N(1), and N(2). One triangular face of the prism is composed of C(25), C(26), and C(27). The second triangular face is composed of N(1), N(2), and P(2). The compound approaches C_s symmetry, with an approximate mirror plane of symmetry defined by P(1), Ta(1), C(25), and P(2). A twist in the P_2N_2 ligand, however, reduces the symmetry and directs the phenyl ring attached to P(1) in the direction of C(26); thus, all the metal-bound methyl groups are inequivalent, with Ta−C bond lengths of 2.239(3), 2.272(3), and 2.252(4) Å.

As has been found for other $[P_2N_2]$ complexes of the early transition elements, the metal is perched on, rather than nested in, the macrocycle.[23,25] The larger P−Ta−P bite angle of 143.00(3)° compared to the smaller N−Ta−N bite angle of 96.39(9)° is consistent with the previously observed binding of the $[P_2N_2]$ ligand in which the amide nitrogens are typically *cis* and the phosphines closer to a *trans* disposition. The capping phosphine Ta−P(1) distance of 2.6180(8) Å is only marginally longer than the Ta−P(2) distance of 2.6088(9) Å. The Ta−N(1) bond length of 2.141(3) Å is shorter than the Ta−N(2) distance of 2.210(2) Å; both of these Ta−N distances are longer than those previously reported[27−31] with the electronically similar amide $N(SiMe_3)_2$, where Ta−N distances have been found in the range of 1.899−2.045 Å. However, none of these compounds contain seven-coordinate tantalum. Therefore, it is uncertain whether these somewhat longer bonds are due to steric crowding or to electronic effects,

Table 1. Crystal Data and Structure Refinement Details for 1 and 2

	1[a]	**2**[b]
formula	$C_{30}H_{58}N_2P_2Si_4Ta$	$C_{26}H_{47}N_2P_2Si_4Ta$
fw	802.04	742.91
color, habit	yellow, plate	orange, irregular
cryst size, mm	0.15 × 0.40 × 0.50	0.50 × 0.25 × 0.25
cryst syst	triclinic	tetragonal
space group	$P\bar{1}$ (No. 2)	$P4_3$ (No. 78)
a, Å	11.6459(14)	16.293
b, Å	15.6915(14)	
c, Å	11.1320(12)	12.785
α, deg	97.591(8)	90
β, deg	95.032(10)	90
γ, deg	107.928(8)	90
V, Å^3	19000.7(4)	3394.1(10)
Z	2	4
T, °C	21.0	−93
ρ_{calcd}, g/cm^3	1.401	1.449
$F(000)$	822.00	1504.00
radiation	Mo	Mo
μ, cm^{-1}	31.19	34.75
transmissn factors	0.634−1.000	0.8093−1.0000[c]
scan type	ω-2θ	ω
scan range, deg in ω	1.31 + 0.35 tan θ	0.5
scan speed, deg/min	32 (up to 9 rescans)	
data collected	$\pm h,\pm k,\pm l$	full sphere
$2\theta_{max}$, deg	70	60.0
cryst decay, %	negligible	negligible
total no. of rflns	17 299	27 691
no. of unique rflns	16 632	4868
R_{merge}	0.038	0.043
no. of rflns with $I \geq n\sigma(I)$	9031	5278
no. of variables	353	313
R	0.031[a]	0.077[b]
R_w	0.027[a]	0.070[b]
GOF	1.39	2.61
max Δ/σ	0.06	0.02
residual density, e/Å^3	−1.11 (near Ta), 0.54	4.53, −5.36 (both near Ta)

[a] Conditions and definitions: Rigaku AFC6S diffractometer, $R = \Sigma||F_o| - |F_c||/\Sigma|F_o|$; $R_w = (\Sigma w(|F_o| - |F_c|)^2/\Sigma w|F_o|^2)^{1/2}$. [b] Conditions and definitions: Rigaku/ADSC CCD diffractometer, $R = \Sigma||F_o^2| - |F_c^2||/\Sigma|F_o^2|$; $R_w = (\Sigma w(|F_o^2| - |F_c^2|)^2/\Sigma w|F_o|^4)^{1/2}$. [c] Includes corrections for decay and absorption.

(25) Fryzuk, M. D.; Love, J. B.; Rettig, S. J. *J. Am. Chem. Soc.* **1997**, *119*, 9071−9072.
(26) Juvinall, G. L. *J. Am. Chem. Soc.* **1964**, *86*, 4202.

such as lack of metal orbitals with sufficient overlap for bonding with the amido π-electrons.

Variable-Temperature NMR Spectroscopy of $[P_2N_2]TaMe_3$ (1). The room-temperature ^1H and ^{31}P NMR spectra of trimethyl species **1** are not indicative of the lack of symmetry observed in the solid-state structure. At room temperature a singlet is observed in the ^{31}P NMR spectrum at δ 30.4. As the temperature is lowered, this ^{31}P NMR signal broadens and then decoalesces at 220 K. The low-temperature limiting spectrum at 180 K consists of two doublets at δ 41.1 and 19.6, with $^2J_{PP} = 71.8$ Hz, which is consistent with two different phosphorus-31 environments with both phosphines bound to the metal center, as observed in the solid state. A line-shape analysis of the variable-temperature ^{31}P NMR spectra from 180 to 230 K combined with an Eyring plot of the resultant rate constants provided the activation parameters of $\Delta H^{\ddagger} = 49.3 \pm 1.5$ kJ mol^{-1} and $\Delta S^{\ddagger} = 57.7 \pm 3.6$ J mol^{-1} K^{-1} for the exchange of the phosphorus environments.

A variable-temperature ^1H NMR study of **1** was also undertaken. At room temperature there is only one signal for the tantalum-bound methyl groups. The chemical shift of this signal is solvent-dependent; it appears at δ 1.14 in C_6D_6 and at δ 0.45 in CD_2Cl_2. The $[P_2N_2]$ ligand in **1** gives rise to two resonances for the silyl methyl groups at room temperature, corresponding to the "top" and "bottom" of the ligand (top refers to the side of the ligand to which the metal is coordinated), and similarly only two signals for the diastereotopic ligand CH_2 protons are observed. The *o*-protons of the phenyl rings give rise to only one resonance, consistent with the single phosphorus environment seen in the room temperature ^{31}P NMR spectrum. The first peak to broaden significantly upon cooling a CD_2Cl_2 solution is that due to the $TaCH_3$ groups; coalescence occurs near 210 K, though the broad peak is difficult to observe, as it overlaps with the silyl methyl peaks. At 200 K, the lowest frequency silyl methyl peak is significantly broadened, and the ligand CH_2 region is composed of a relatively sharp multiplet integrating to four protons, and a broad peak centered about the same region, due to the remaining four ligand CH_2 protons. By 180 K many of the features of the spectrum are beginning to sharpen but are still broad. There are four silyl methyl signals, as well as four ligand CH_2 environments. There are also two ortho protons, as anticipated from the low-temperature ^{31}P NMR spectrum. The tantalum-bound methyl groups appear as two broad peaks, a peak at δ 0.81 integrating to one methyl group and a second at δ 0.17 integrating for the remaining two methyl groups. The absence of a low-temperature limiting spectrum makes the determination of activation parameters for the fluxional processes of **1** from ^1H NMR measurements less reliable than those obtained from ^{31}P NMR data. It is clear, however, that the low-temperature ^1H spectrum is consistent with a molecule of C_s symmetry, with one metal-bound methyl, two phosphorus nuclei, and the tantalum center defining a mirror plane, as would be expected for a capped-trigonal-prismatic geometry. Nevertheless, the low-temperature solution structure, as determined by NMR spectroscopy to be of C_s symmetry, and the solid-state structure do not quite match; the twist in the ligand framework observed in the solid state is not evident from the solution data even at 180 K, which suggests that the macrocyclic $[P_2N_2]$ ligand framework must be conformationally flexible.

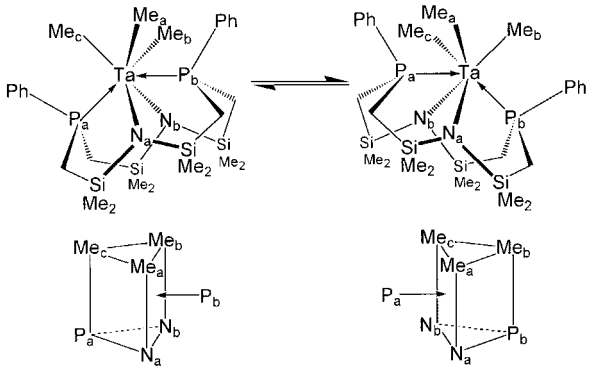

Figure 2. Fluxional behavior of capped-trigonal-prismatic **1** in solution. Tantalum methyl groups exchange sites in the trigonal prism by rotating in a turnstile manner while the ligand simultaneously pivots, exchanging phosphine environments. Only Me_a is in a chemically identical environment, remaining on a phosphine-capped face; one further rotation of the $TaMe_3$ fragment in the same direction exchanges the Me_a environment.

The mechanism of the exchange between the two phosphorus environments and the exchange between the two $TaCH_3$ environments can be rationalized via a pseudo "turnstile" mechanism, where the three $TaCH_3$ groups rotate with simultaneous exchange of the two phosphorus environments, as shown in Figure 2. The low value of $\Delta S^{\ddagger}$ is inconsistent with a dissociative mechanism where a phosphine dissociates prior to rotation. That **1** is fluxional is expected, considering the small energy differences between the various seven-coordinate metal geometries, and a similar $\Delta G^{\ddagger}$ value has been found in related seven-coordinate systems.[19] The $[P_2N_2]$ ligand must be quite flexible to accommodate such changes in geometry.

Photolysis of $[P_2N_2]TaMe_3$ and Structure of $[P_2N_2]Ta{=}CH_2(Me)$ (2). The trimethyl **1** is more thermally stable than its precursor, $TaMe_3Cl_2$. Solutions of **1** are light-sensitive, however, converting to the orange methyl methylidene $[P_2N_2]Ta{=}CH_2(Me)$ (**2**) with loss of methane (detected by GC-MS) upon photolysis (eq 2). Indicative of the formation of a methylidene is a resonance integrating to two protons at δ 9.18 in the ^1H NMR spectrum, as well as a signal in the ^{13}C NMR spectrum at δ 244.8, typical of tantalum methylidene

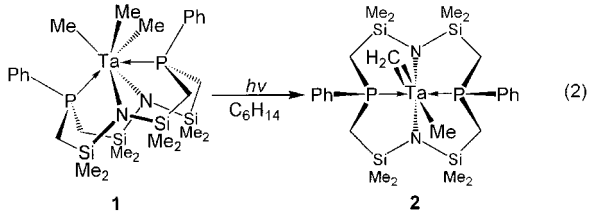

(2)

1 **2**

(27) Hoffman, D. M.; Suh, S. *J. Chem. Soc., Chem. Commun.* **1993**, 714−715.
(28) Bradley, D. C.; Hursthouse, M. B.; Howes, A. J.; Jelfs, A. N. d. M.; Runnacles, J. D.; Thornton-Pett, M. *J. Chem. Soc., Dalton Trans.* **1991**, 841−847.
(29) Bradley, D. C.; Hursthouse, M. B.; Malik, K. M. A.; Nielson, A. J.; Vuru, G. B. C. *J. Chem. Soc., Dalton Trans.* **1984**, 1069−1072.
(30) Suh, S.; Hoffman, D. M. *Inorg. Chem.* **1996**, *35*, 5015−5018.
(31) Bradley, D. C.; Hursthouse, M. B.; Malik, K. M. A.; Vuru, G. B. C. *Inorg. Chim. Acta* **1980**, *44*, L5-L6.

complexes. The aforementioned ^{13}C NMR signal shows a 118 Hz $^1J_{HC}$ value which is lower than those observed for $(\eta^5\text{-}C_5H_5)_2Ta{=}CH_2(Me)$ ($^1J_{HC}$ = 132 Hz) and $(\eta^5\text{-}C_5Me_5)_2Ta{=}CH_2(Me)$ ($^1J_{HC}$ = 127 Hz) but very similar to that observed for $[PhC(NSiMe_3)_2]_2Ta{=}CH_2(Me)$ ($^1J_{CH}$ = 118 Hz).

This transformation occurs under ordinary fluorescent light over several weeks or, more conveniently, by exposure of solutions of **1** to direct sunlight or a sunlamp. Ordinary incandescent light results in no conversion, and stronger UV sources result in decomposition. As has been suggested by others for a similar reaction,[20,21] the mechanism of this reaction presumably involves charge transfer from a methyl group to the metal center, producing a methyl radical that then readily abstracts a hydrogen atom from an adjacent methyl group, thus eliminating methane and producing a methylidene moiety. Photochemical α-hydrogen abstraction has been noted before for both the early and late transition metals.[20,21,32,33] UV−vis spectroscopy of **1** in hexanes shows two absorptions in the region expected for a ligand-to-metal charge-transfer band corresponding to an alkyl-to-metal charge transfer, at wavelengths of 262 and 322 nm.

Although NMR spectroscopy indicates that methylidene **2** is the major product of the reaction with only trace NMR-active impurities, performing the photolysis on an NMR scale in C_6D_6 with ferrocene as an internal concentration standard demonstrates that side products are produced well before conversion to the methylidene is complete. For example, after 11 min of photolysis the solution turns from yellow to light orange and a 54% conversion to methylidene is observed, and nearly 90% of the initial tantalum content is accounted for from **1** and **2**. A maximum conversion of 60% was observed after 33 min, with only 72% of the initial tantalum content being accounted for by NMR-active products. At this point the solution is dark brown. After 85 min the solution is dark green and the yield of **2** has dropped to 48%, and 64% of the initial tantalum is observed in the ^1H NMR spectrum. EPR spectroscopy of a solution of **1** after 60 min of photolysis under a sun lamp indicates that a tantalum species in oxidation state +4 is present; an eight-line pattern is observed in the EPR spectrum, due to an electron with hyperfine coupling to ^{181}Ta (spin $^7/_2$, 99.99% abundant). Superhyperfine coupling to ^{31}P is also observed, though poorly resolved. This EPR-active product likely results from the photolysis of the methylidene **2** and still contains the $[P_2N_2]$ ligand. Attempts are underway to identify this compound.

Like methylidene **2**, the paramagnetic impurities are highly soluble in relatively nonpolar solvents such as pentane and hexamethyldisiloxane. To generate **2** with a minimum amount of these impurities, short photolysis times and therefore low conversion of the tantalum trimethyl **1** are required. Solubility differences allow **2** to be separated from **1** by rinsing with cold pentane, and the much less soluble **1** can be recovered and recycled.

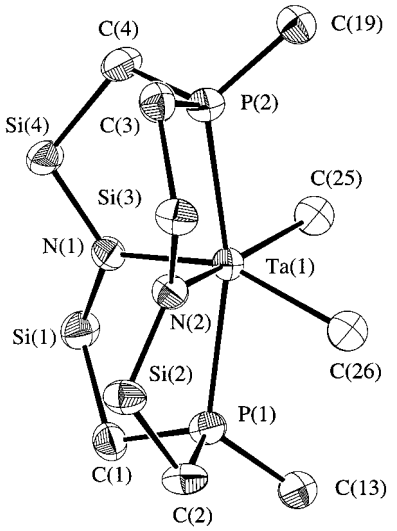

Figure 3. ORTEP representation of the solid-state molecular structure of $[P_2N_2]Ta{=}CH_2(Me)$ (**2**).

Once purified, methylidene **2** is quite thermally stable; solutions of **2** decompose only slowly at room temperature, and as a solid **2** can be stored at −40 °C without noticeable decomposition. Compound **2** is much more soluble in nonpolar solvents than trimethyl **1**; for example, methylidene **2** is extremely soluble in hexanes, pentane, and even hexamethyldisiloxane. Due to this high solubility, crystals of **2** suitable for X-ray analysis could only be obtained by slow evaporation of a pentane solution at −40 °C, as other higher boiling solvents gave only waxy products. The solid-state structure of **2** is shown in Figure 3, and crystallographic data are given in Table 1.

The solid-state structure verifies that **2** is monomeric. Similar to a tantalum methyl methylidene recently reported,[19] the structure of **2** shows disorder. The metal-bound methyl and methylidene ligands were modeled as 1:1 2-fold disordered; as a result, the metal−methylidene Ta−C(25) distance of 2.09(2) Å and metal−methyl Ta−C(26) distance of 2.21(2) Å have large errors associated with them.

The two geometries previously reported for six-coordinate species containing the $[P_2N_2]$ ligand are exemplified by $[P_2N_2]ZrCl_2$ and $[P_2N_2]Zr(CH_2Ph)_2$.[23] In the former the chloride ligands, the zirconium center, and the two amido ligands lie in a plane, and thus the complex is approximately octahedral. In the dibenzylzirconium species the dibenzyl ligands and the zirconium center define a plane that approximately bisects the two planes defined by N−Zr−N and P−Zr−P, producing what is best described as a distorted-trigonal-prismatic species. As the geometry of methylidene **2** is intermediate between these two cases, it can therefore be considered intermediate between octahedral and trigonal prismatic. While the trigonal-prismatic geometry is electronically preferred by early-metal alkyl compounds over the octahedral geometry,[34−38] the intermediate

(32) Edwards, D. S.; Blondi, L. V.; Ziller, J. W.; Churchill, M. R.; Schrock, R. R. *Organometallics* **1983**, *2*, 1505.
(33) Fryzuk, M. D.; MacNeil, P. A.; Rettig, S. J. *J. Am. Chem. Soc.* **1985**, *107*, 6708.
(34) Kang, S. K.; Tang, H.; Albright, T. A. *J. Am. Chem. Soc.* **1993**, *115*, 1971.
(35) Rodriguez, G.; Bazan, G. C. *J. Am. Chem. Soc.* **1995**, *117*, 10155−10156.
(36) Haaland, A.; Hammel, A.; Rypal, K.; Volden, H. V. *J. Am. Chem. Soc.* **1990**, *112*, 4547.
(37) Morse, P. M.; Girolami, G. S. *J. Am. Chem. Soc.* **1993**, *115*, 1971.

Scheme 1

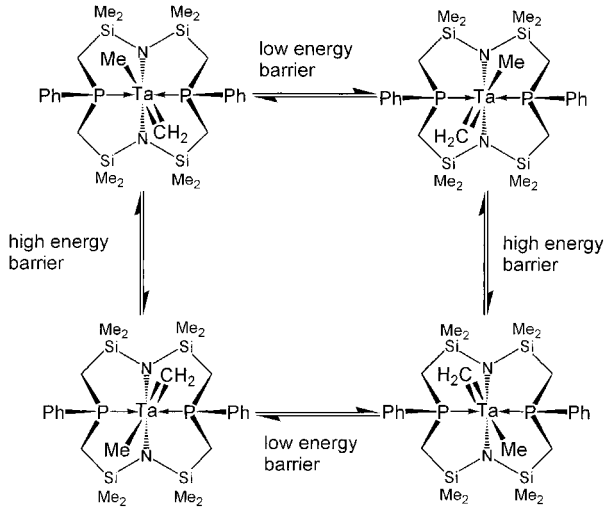

geometry observed here may be rationalized by the preference of the methylidene fragment for a more octahedral geometry, to maximize π-bonding of the methylidene p orbital with the tantalum d orbitals. This is discussed in more detail below.

The ligand geometry once again contains approximately *trans* phosphines with a P−Ta−P angle of 165.11(7)° and *cis* amides with a N−Ta−N angle of 114.1(5)°. The Ta−P(1) distance of 2.550(2) Å and Ta−P(2) distance of 2.542(2) Å are shorter than those for seven-coordinate **1**. The Ta−N(1) and Ta−N(2) distances of 2.146(6) and 2.142(6) Å are comparable to those seen in **1**.

Fluxional Processes of $[P_2N_2]Ta{=}CH_2(Me)$. The ^{31}P NMR spectrum of methylidene **2** is a singlet at 300 K and is unchanged over the temperature range of 160−330 K; the distorted-trigonal-prismatic geometry observed in the solid state is therefore not rigid in solution. Both the $Ta{=}CH_2$ and $Ta{-}CH_3$ groups must readily pass through the plane that contains the amido ligands and the tantalum center, with an inconsequential barrier resulting from the octahedral intermediate. This motion renders the phosphorus-31 environments identical, and thus we expect the ^1H NMR spectrum to reflect a species with apparent C_s symmetry. This fluxional process is depicted by the horizontal equilibria in Scheme 1.

The second fluxional process, depicted as the vertical equilibria in Scheme 1, is observed in the ^1H NMR spectra close to room temperature. At low temperatures (180−260 K), there are four sharp resonances observed for the silyl methyl groups of the ligand, and four ligand CH_2 environments, as expected from a $[P_2N_2]$ complex with apparent C_s symmetry in solution. When the temperature is raised, however, the silyl methyl and ligand methylene resonances begin to broaden and separately coalesce, until two silyl methyl and two ligand methylene peaks remain (~340 K; decomposition becomes significant at higher temperatures and impurities obscure relevant peaks). These observations indicate that there is some mechanism by which the position of the methyl and methylidene ligands can exchange.

An EXSY spectrum of **2** shows no positively phased cross-peak between the tantalum-bound methyl group protons and methylidene protons. Likewise, 1-D saturation transfer experiments show only nuclear Overhauser effects between the tantalum methyl group and methylidene protons, implying that the mechanism of exchange does not involve hydrogen atom transfer from the methyl group to the methylene group. Dimerization would allow for exchange of methylidene fragments, but because coupling from the methylidene protons to the phosphines and methyl protons is maintained at higher temperature, this is not a feasible mechanism. Likewise, the line shape of the silyl methyl resonances is not affected by concentration, as would be anticipated if a second-order dimerization mechanism was active. The most probable mechanism therefore must involve rearrangement of the ligand to allow rotation of the $Ta{=}CH_2$ and $TaCH_3$ groups with respect to the $[P_2N_2]$ ligand. From line-shape analysis of the silyl methyl peaks in the ^1H NMR spectrum from 280 to 320 K it was possible to obtain kinetic parameters for this exchange process of $\Delta H^{\ddagger} = 58.6 \pm 1.2$ kJ mol^{-1} and $\Delta S^{\ddagger} = -16.7 \pm 2.1$ J mol^{-1} K^{-1}. The small entropy of activation is consistent with an intramolecular mechanism, without any prior ligand dissociation. For rotation to occur, the phosphine ligand must become more *cis*-disposed, and the amido ligands must assume a more *trans* disposition. This indicates that the bound $[P_2N_2]$ fragment must be quite flexible; the rearrangement from *cis*-disposed amido ligands to *trans* amido ligands must be assisted by the distortion from ideal octahedral angles imposed due to the macrocyclic nature of the ligand.

A third fluxional process observed by variable-temperature ^1H NMR spectra involves rotation of the methylidene unit. In the ^1H NMR spectrum of **2** at 300.2 K the methylidene and methyl fragments are broad multiplets. However, using Lorentz−Gaussian enhancement it was possible to resolve the 1.2 Hz coupling between the methylidene and methyl fragment, as well as coupling of both signals to two identical phosphorus-31 environments. The presence of only one methylidene resonance is due to the rapid rotation of the methylidene unit. Cooling initially causes some loss of resolution of both the methyl and methylidene resonance and obvious broadening of the methylidene signal. Decoalescence of the methylidene resonance occurs at approximately 190 K, and further cooling to 170 K leads to two resonances for the methylidene protons, separated by 1.08 ppm; this separation does not change upon additional cooling to 160 K. The resolution at this temperature was not adequate to distinguish the anticipated couplings in these resonances.

The calculated $\Delta G^{\ddagger}$ value for the rotation of the methylidene group from this NMR data is 33.5 ± 0.6 kJ mol^{-1} at 190 K; this value is significantly lower than that previously observed for $(\eta^5\text{-}C_5H_5)_2Ta{=}CH_2(Me)$, for which $\Delta G^{\ddagger}$ for rotation of the methylidene group was estimated to be larger than 89.5 kJ mol^{-1}.[2] This large difference is due to the availability of two perpendicular d orbitals for π-bonding. Whereas $(\eta^5\text{-}C_5H_5)_2Ta{=}CH_2\text{-}(CH_3)$ is an 18e$^-$ complex, with only one orbital of correct symmetry for π-bonding,[4] **2** may be considered a 14e$^-$ species, excluding π donation from the two amido

(38) Gillespie, R. J.; Robinson, E. A. *Angew. Chem., Int. Ed. Engl.* **1996**, *35*, 495−514.

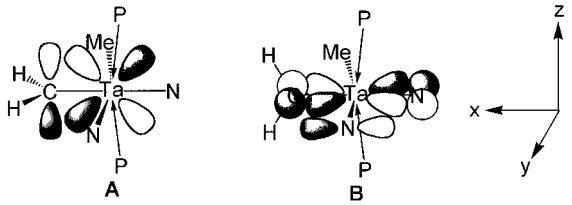

Figure 4. Representations of two possible orientations of the Ta=CH_2 double bond in $[P_2N_2]$Ta=CH_2(Me) (**2**). Competition with the π-donor amido ligands for the d_{xy} orbital disfavors **B**.

nitrogens. The two extreme arrangements of the Ta=CH_2 unit in an approximately octahedral complex are shown in Figure 4, along with the d orbitals available for π-bonding. In conformation **A,** the methylidene hydrogens are in the same plane as the amido nitrogens; thus, the p orbital on the methylidene carbon overlaps with the d_{xz} orbital. In **A,** two methylidene proton environments exist, as observed in the low-temperature ^{1}H NMR spectrum. Another possible conformation, **B**, has the methylidene unit rotated 90°; the d_{xy} orbital now has the correct symmetry for overlap with the methylidene carbon p orbital. The macrocyclic ligand restricts the possible orientations of the lone pair containing p orbitals of the amido nitrogens, and therefore the d_{xy} orbital is also the only orbital of correct symmetry for reasonable overlap with these orbitals. As a result, in conformation **B** the methylidene π-electrons must compete with the two amido donors for the d_{xy} orbital, and this is therefore predicted to be a less favorable orientation of the methylidene unit. This is in agreement with the experimental data, since in the second conformation the two methylidene protons are identical, contrary to what is observed in the low-temperature-limit ^{1}H NMR spectrum. It is interesting to note that because the two amido p-orbitals compete for one orbital for π-donation to tantalum, **2** can be no more than a 16e$^-$ species.

Synthesis and Deprotonation of $\{[P_2N_2]TaMe_2\}^+X^-$ ($X = BF_4^-$, $B(C_6F_5)_4^-$). The precedented chemical route to tantalum methylidenes involves the deprotonation of cationic methyl compounds, as exemplified by the synthesis of (η^5-$C_5H_5)_2$Ta=CH_2(Me) by treatment of $\{Cp_2TaMe_2\}^+BF_4^-$ with the base $Me_3P{=}CH_2$.[1,3,19] A similar route to **2** would be desirable, to avoid the paramagnetic side products that are generated by photolysis of **1** at high conversion.

The reaction of **1** with $Ph_3C^+BF_4^-$ in CH_2Cl_2 produces $\{[P_2N_2]TaMe_2\}^+BF_4^-$ (**3**), which is soluble in both CH_2Cl_2 and THF (eq 3). Solutions of **3** are not thermally

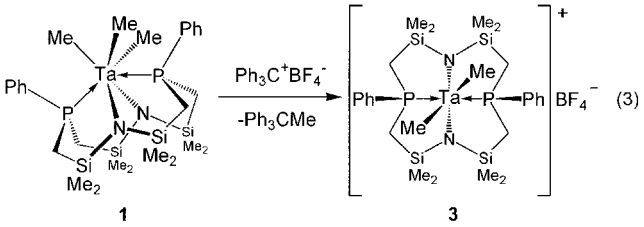

(3)

stable; decomposition in CH_2Cl_2 is complete after 3 days at room temperature and results in a colorless crystalline precipitate. The stability of the cation in **3** is improved by using a less reactive anion. The reaction of $\{PhNMe_2H\}^+B(C_6F_5)_4^-$ with **1** produces $\{[P_2N_2]$-$TaMe_2\}^+B(C_6F_5)_4^-\cdot PhNMe_2$ (**4**) (eq 4), which does not decompose after several days in solution.

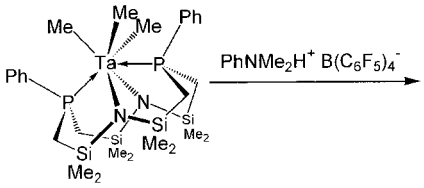

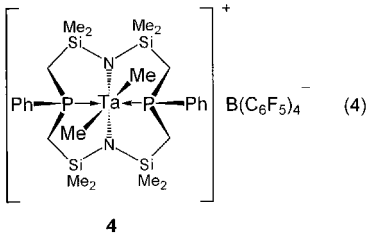

(4)

The ^{1}H and ^{31}P NMR spectra of the $\{[P_2N_2]TaMe_2\}^+$ ion in **3** and **4** are nearly identical, though the $PhNMe_2$ byproduct proved impossible to remove from **4** even under high vacuum. The similarity between the ^{1}H NMR spectra of **3** and **4** is evidence that the $PhNMe_2$ molecule in **4** is not coordinated to the metal center. The low-temperature ^{31}P NMR spectra also provide evidence that the $PhNMe_2$ byproduct is not coordinated. A single phosphorus environment is observed for $\{[P_2N_2]TaMe_2\}^+$ from room temperature to 185 K, unlike the seven-coordinate trimethyl **1**, which had two coupled signals at low temperature. The low-temperature (200 K) ^{1}H NMR spectrum of **4** shows a single tantalum methyl signal and four silyl methyl environments, consistent with a trigonal-prismatic geometry at tantalum; an octahedral geometry would be expected to have only two silyl methyl signals. However, at room temperature the ^{1}H NMR spectrum of **4** shows only two silyl methyl environments (apparent C_{2v} symmetry), indicating a relatively small energy difference between the trigonal-prismatic geometry and the octahedral transition state that exchanges the silyl methyl environments.

Deprotonation of **3** or **4** did not prove to be a successful alternative route to the methylidene methyl **2**. The reaction of the bulky amides $LiNPr^i_2$ and $NaN(SiMe_3)_2\cdot$THF with the BF_4^- salt **3** instead generated $[P_2N_2]$-$TaMe_2F$ (**5**) as the major product (eq 5). The room-

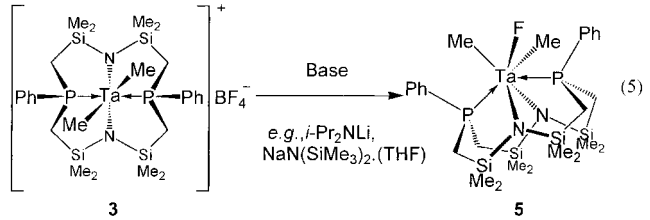

(5)

temperature ^{31}P NMR spectrum of **5** is indicative of the formation of a tantalum fluoride; a single doublet is observed due to coupling to ^{19}F. The methyl groups are equivalent in the ^{1}H NMR spectrum and show coupling to two ^{31}P nuclei and a ^{19}F nucleus. The fluxional process seen in seven-coordinate **5** is similar to that observed for **1**; at the low-temperature limit the ^{31}P NMR spectrum of **5** consists of two coupled signals, one at δ 26.5, the other at δ 43.9, consistent with the capped-

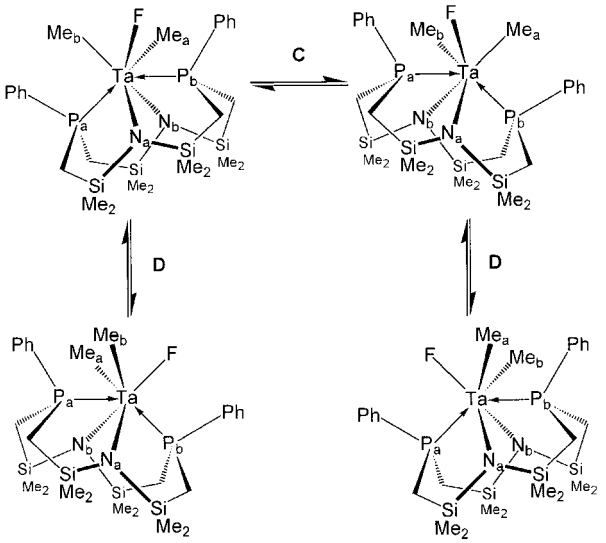

Figure 5. Fluxional processes in $[P_2N_2]TaMe_2F$ (**5**).

trigonal-prismatic geometry observed for **1**. The variable-temperature ^1H NMR spectra are more complicated. Warming the sample to 360 K produces a species with two silyl methyl environments and one tantalum methyl group, as was observed in the room-temperature spectrum of **1** and was explained by the rotation of the methyl groups with simultaneous pivoting of the $[P_2N_2]$ ligand. Four environments are observed for the silyl methyl groups of **5** at 240 K, and further cooling shows that they begin to decoalesce again, to give eight silyl methyl environments. This is consistent with a low-temperature structure lacking a mirror plane of symmetry, and therefore the fluorine atom must lie in one of the two equivalent sites eclipsing the nitrogen atoms in the trigonal prism and does not occupy the site in the trigonal prism that lies in a plane with the two phosphorus atoms and tantalum center. This lowest energy structure is depicted as the top left and top right structures in Figure 5. The variable-temperature ^1H NMR spectra observed are consistent with exchange of the fluoride between these two equivalent sites on the NMR time scale in the ^1H spectra at 240 K, where four silyl methyl environments are observed, but the fluoride does not exchange with the third site. This corresponds to equilibrium **C** in Figure 5. The complete rotation of the two methyl and fluoride groups is only observed at higher temperature and leads to the two silyl methyl groups observed at 360 K, depicted as the fluxional process **D** in Figure 5.

The use of $Me_3P{=}CH_2$ as a base for the deprotonation of **3** resulted in a new major product, **6**, with two singlets in the ^{13}P NMR spectrum: one in the region typical of the bound $[P_2N_2]$ and a second signal closer to the unbound ligand (eq 6). Compound **5** was observed as a minor impurity. The ^1H NMR spectrum of **6** is indicative of a highly unsymmetrical species, with eight silyl methyl resonances, two of which show coupling to phosphorus. While eight signals are expected for the ligand methylene groups, only seven are observed. One is at unusually high frequency and shows only coupling to the two ^{31}P nuclei. These data indicate that **6** is the result of the deprotonation of **3** not at a tantalum methyl group but rather at a methylene group of the $[P_2N_2]$ ligand. The reaction of $LiNPr^i_2$, $NaN(SiMe_3)_2{\cdot}THF$, or

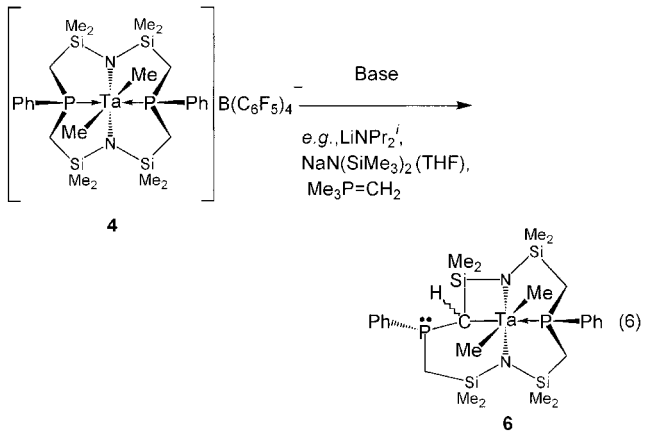

$Me_3P{=}CH_2$ with **4** also produced **6** as the major product. The exact stereochemistry of the product is unknown, though as there is only one product, the base appears to selectively deprotonate only one of the two possible diastereotopic methylene protons.

Conclusions

The results of this study indicate that the $[P_2N_2]$ macrocycle is a useful alternative to the ubiquitous η^5-C_5H_5 ligand and can be used to stabilize a number of organometallic complexes of Ta(V). The seven-coordinate trimethyl derivative $[P_2N_2]TaMe_3$ is fluxional and can be used as a starting material for other organotantalum complexes. For example, photolysis of $[P_2N_2]$-$TaMe_3$ leads to the methylidene derivative $[P_2N_2]Ta{=}CH_2(Me)$; with excessive photolysis paramagnetic species are also produced. The methylidene is fluxional as well, although in this case, there are at least three processes that are operating. In an effort to improve the yields of the methylidene complex, a nonphotochemical route was attempted. First the trimethyl species was converted to the dimethyl cation $\{[P_2N_2]TaMe_2\}^+$ by reaction with Ph_3C^+. Attempts to form the methylidene complex from the dimethyl cation by deprotonation failed in different ways, depending on the anion used to stabilize the starting cation and the base used. If the anion was BF_4^-, reaction with strong bases led to incorporation of fluoride and the formation of $[P_2N_2]TaMe_2F$. If the anion was $B(C_6F_5)_4^-$, reaction with strong bases did involve deprotonation but not at the Ta−Me groups; instead, deprotonation occurred at the methylene protons of the macrocyclic framework. This latter reaction path indicates one of the drawbacks of this ligand system; the relatively acidic methylene protons can be deprotonated even in the presence of the sterically more accessible Ta−Me group.

Experimental Section

Unless otherwise stated, all manipulations were performed under an atmosphere of dry oxygen-free dinitrogen by means of standard Schlenk or glovebox techniques (Vacuum Atmospheres HE-553-2 glovebox equipped with a MO-40-2H purification system and a −40 °C freezer). Hexanes were predried by refluxing over CaH_2 and then distilled under argon from sodium benzophenone ketyl with tetraglyme added to solubilize the ketyl. Anhydrous diethyl ether was stored over sieves and distilled from sodium benzophenone ketyl under argon. Toluene was predried by refluxing over CaH_2 and then distilled

from sodium under argon. Nitrogen was dried and deoxygenated by passing the gases through a column containing molecular sieves and MnO. Deuterated benzene and toluene were dried by refluxing with molten potassium metal and molten sodium metal, respectively, in a sealed vessel under partial pressure, then trap-to-trap-distilled, and freeze−pump−thaw-degassed three times. Deuterated methylene chloride was dried over CaH_2 prior to use. Unless otherwise stated, ^1H, ^{31}P, $^1H\{^{31}P\}$, $^{13}C\{^1H\}$, ^{13}C, and variable-temperature NMR spectra were recorded on a Bruker AMX-500 instrument operating at 500.1 MHz for ^1H spectra. ^1H NMR spectra were referenced to internal C_6D_5H (δ 7.15), $CDHCl_2$ (δ 5.32), and C_7D_7H (δ 2.09), $^{31}P\{^1H\}$ NMR spectra to external $P(OMe)_3$ (δ 141.0 with respect to 85% H_3PO_4 at δ 0.0), and ^{13}C NMR spectra to $^{13}CC_5D_6$ (δ 128.4) and $^{13}CD_2Cl_2$ (δ 54.0). Simulation of variable-temperature NMR spectra were performed using the program DNMR-SIM.[39] Simulated and actual spectra were compared by peak widths at half-height. UV−vis spectra were obtained using a Hewlett-Packard 8453 UV−visible spectrophotometer and quartz cuvettes with Teflon valves. ESR spectra were recorded on a Bruker ECS 106. Elemental analyses were performed by Mr. P. Borda of this department.

The compounds *syn*-$[P_2N_2]Li_2.C_4H_8O_2$[22] and $TaMe_3Cl_2$[3] were prepared according to literature procedures. Lithium diisopropylamide was purchased from Aldrich.

Preparation of $[P_2N_2]TaMe_3$ (1). A solution of $TaMe_3Cl_2$ (5.214 g, 17.56 mmol) in 40 mL of ether was added to a stirred solution of $[P_2N_2]Li_2{\cdot}C_4H_8O_2$ (11.147 g, 17.56 mmol) in 1 L of ether at −78 °C. The solution was shielded from light because the product is light-sensitive. The resulting yellow solution was warmed slowly to 0 °C, over which time a white precipitate formed. The solution was evaporated to dryness. The resulting solid was extracted into 50 mL of toluene and filtered and the solvent removed. The remaining solids were rinsed with a minimal amount of hexanes and thoroughly dried under vacuum, yielding $[P_2N_2]TaMe_3$ as a yellow powder in 80% yield. X-ray-quality crystals that contained 0.5 equiv of cocrystallized hexanes were obtained by cooling a saturated hexanes solution to −40 °C; drying under vacuum generated solvent-free material. ^1H NMR (500 MHz, C_6D_6, 25 °C): δ 0.33 and 0.34 (s, 24H total, SiCH_3), 1.14 (t, $^2J_{PH}$ = 6.5 Hz, 9H, TaCH_3), 1.48 and 1.52 (AMX, $^2J_{HH}$ = 14.3 Hz, 8H, CH_2 ring), 7.07 (m, 6H, *m*/*p*-*H*), 7.65 (m, 4H, *o*-*H*). $^{31}P\{^1H\}$ NMR (81.0 MHz, C_6D_6, 25 °C): δ 30.4 (s). $^{31}P\{^1H\}$ NMR (81.0 MHz, C_7D_8, −93 °C): δ 19.6 (d, $^2J_{PP}$ = 71.8 Hz), 41.1 (d, $^2J_{PP}$ = 71.8 Hz). ^{13}C NMR (50.3 MHz, C_6D_6, 25 °C): δ 5.7 (s, SiCH_3), 8.37 (t, SiCH_3), 20.3 (s, PCH_2Si), 64.8 (s, TaCH_3), 129.7, 131.8 and 137.5 (Ph-*C*). UV−vis: λ_{max} (ϵ_M) 262 (12 500), 322 (6220), 399 (sh) nm. Anal. Calcd for $C_{27}H_{51}N_2P_2Si_4Ta$: C, 42.73; H, 6.77; N, 3.69. Found: C, 42.61; H, 6.87; N, 3.73.

Preparation of $[P_2N_2]Ta{=}CH_2(Me)$ (2). A yellow solution of $[P_2N_2]TaMe_3$ (0.75 g, 0.99 mmol) in 200 mL of hexanes was irradiated for 15 min using an Osram Ultra-Vitalux sunlamp, resulting in an orange solution. The solvent was removed, and the remaining waxy solid was extracted into 10 mL of pentane. The pentane solution was cooled to −40 °C and then filtered. The solvent was removed and the sample dried thoroughly in vacuo, yielding $[P_2N_2]Ta(CH_2)CH_3$ (0.33 g, 45%) as an orange solid. The filtered solid was mostly unconverted $[P_2N_2]TaMe_3$. X-ray-quality single crystals were obtained by slow evaporation of a pentane solution at −40 °C. ^1H NMR (500 MHz, C_7D_8, 260 K): δ 0.14, 0.16, 0.20, and 0.27 (s, 24H total, SiCH_3), 0.75 (tt, $^3J_{HP}$ = 3.3 Hz, $^4J_{HH}$ = 1.2 Hz, 3H, TaCH_3), 1.11 (dd, $^2J_{HH}$ = 13.7 Hz, J_{HP} = 5.8 Hz, 2H, CH_2 ring), 1.32 (dd, $^2J_{HH}$ = 13.7 Hz, J_{HP} = 5.2 Hz, 2H, CH_2 ring), 1.36 and 1.36 (t, J_{HP} = 5.8 Hz, 4H, CH_2 ring), 7.15 (m, 2H, *p*-*H*), 7.22 (m, 4H, *m*-*H*), 8.03 (m, 4H, *o*-*H*), 9.18 (tq, $^3J_{HP}$ = 3.0 Hz, $^4J_{HH}$ = 1.2 Hz, 2H, TaCH_2). $^{31}P\{^1H\}$ NMR (81.0 MHz, C_6D_6, 25 °C): δ 27.3 (s). $^{13}C\{^1H\}$ NMR (125.8 MHz, C_6D_6, 25 °C): δ 4.9, 5.1, 5.8, 6.0 (br, SiCH_3), 20.9 and 20.7 (br, SiCH_2P), 84.4 (t, $^2J_{PC}$ = 9.3 Hz, TaCH_3), 128.7 (t, J_{PC} = 5.0 Hz, PPh-*C*), 130.1 (s, PPh-*C*), 132.9 (t, J_{PC} = 6.5 Hz, PPh-*C*), 138.2 (t, $^1J_{PC}$ = 17.7 Hz, *o*-*C*), 244.8 (t, $^2J_{PC}$ = 8.9 Hz, TaCH_2). ^{13}C NMR (125.8 MHz, C_6D_6, 25 °C): δ 244.8 (m, $^1J_{HC}$ = 119 Hz, TaCH_2). Anal. Calcd for $C_{26}H_{47}N_2P_2Si_4Ta$: C, 42.04; H, 6.38; N, 3.77. Found: C, 42.34; H, 6.44; N, 3.65.

$\{[P_2N_2]TaMe_2\}^+BF_4^-$ (3). To a stirred solution of **1** (5.087 g, 6.702 mmol) in 80 mL of CH_2Cl_2 cooled to −78 °C was added a solution of $Ph_3C^+BF_4^-$ (2.213 g, 6.702 mmol) in 30 mL of CH_2Cl_2. The mixture was warmed to room temperature, and the solution was filtered to remove a trace precipitate. The solvent was removed, providing a white solid, which was thoroughly rinsed with toluene. The solid was dried under vacuum, yielding $\{[P_2N_2]TaMe_2\}^+BF_4^-$ as a white powder (4.8 g, 86% yield). Solutions of **3** in CH_2Cl_2 decompose over several days at room temperature; therefore, the solid is best stored at −40 °C. ^1H NMR (CD_2Cl_2, 25 °C, 500 MHz): δ 0.40 and 0.54 (s, 24H total, SiCH_3), 1.28 (t, $^2J_{PH}$ = 5.8 Hz, 6H, TaCH_3), 1.66 (dt, $^2J_{HH}$ = 14.9 Hz, $^2J_{HP}$ = 6.6 Hz, 4H, CH_2 ring), 1.84 (dt, $^2J_{HH}$ = 14.9 Hz, $^2J_{HP}$ = 5.4 Hz, 4H, CH_2 ring), 7.54 (m, 10H, P*Ph*-*H*). $^{31}P\{^1H\}$ NMR (CD_2Cl_2, 25 °C, 81.0 MHz): δ 24.2 (s). $^{13}C\{^1H\}$ NMR (CD_2Cl_2, 25 °C, 125.8 MHz): δ 4.7 (s, SiCH_3), 5.2 (br, SiCH_3), 17.9 (br, SiCH_2P), 80.2 (s, TaCH_3), 129.8 (t, J_{PC} = 5.0 Hz, PPh-*C*), 131.8 (s, PPh-*C*), 131.9 (t, J_{PC} = 5.3 Hz, PPh-*C*). Anal. Calcd for $C_{26}H_{48}BF_4N_2P_2Si_4Ta$: C, 37.59; H, 5.82; N, 3.37. Found: C, 37.91; H, 5.99; N, 3.27.

$\{[P_2N_2]TaMe_2\}^+B(C_6F_5)_4^-{\cdot}(C_6H_5NMe_2)$ (4). To a stirred solution of **1** (0.689 g, 0.908 mmol) in 20 mL of CH_2Cl_2 cooled to −78 °C was added $PhNMe_2H^+B(C_6F_5)_4^-$ (0.728 g, 0.908 mmol) in 20 mL of CH_2Cl_2. The solution was warmed to room temperature and the solvent removed. The remaining solid was rinsed with toluene, producing an insoluble oil, which was separated from the toluene layer via pipet and dried under vacuum, yielding **4** as a creamy white powder (1.102 g, 79% yield). ^1H NMR (CD_2Cl_2, 25 °C, 500 MHz): δ 0.40 and 0.54 (s, 24H total, SiCH_3), 1.28 (t, $^2J_{PH}$ = 5.8 Hz, 6H, TaCH_3), 1.66 (dt, $^2J_{HH}$ = 14.9 Hz, $^2J_{HP}$ = 6.6 Hz, 4H, CH_2 ring), 1.84 (dt, $^2J_{HH}$ = 14.9 Hz, $^2J_{HP}$ = 5.4 Hz, 4H, CH_2 ring), 2.92 (s, 6H, PhN(CH_3)$_2$), 6.95 (m, 2H, N*Ph*-*o*-*H*), 7.11 (m, 2H, N*Ph*-*m*-*H*) 7.54 (m, 11H, P*Ph*-*H* and N*Ph*-*p*-*H*). $^{31}P\{^1H\}$ NMR (CD_2Cl_2, 25 °C, 81.0 MHz): δ 24.2 (s). ^1H NMR (500 MHz, CD_2Cl_2, 200 K): δ 0.25, 0.33, 0.40, and 0.47 (s, 24H total, SiCH_3), 1.08 (m, 6H, TaCH_3) 1.16, 1.46, 2.03, and 2.12 (m, 8H total, CH_2 ring), 2.87 (s, 6H, PhN(CH_3)$_2$), 6.62 (t, 1H, NPh-*p*-*H*), 6.66 (m, 2H, NPh-*o*-*H*), 7.17 (m, 2H, NPh-*m*-*H*), 7.44 (m, 4H, PPh-*o*-*H*), 7.54 (m, 6H, PPh-*o*/*m*-*H*). Anal. Calcd for $C_{58}H_{59}BF_{20}N_3P_2Si_4Ta$: C, 45.11; H, 3.85; N, 2.72. Found: C, 45.46; H, 3.79; N, 2.41.

$[P_2N_2]TaMe_2F$ (5). To a slurry of $\{[P_2N_2]TaMe_2\}^+BF_4^-$ (0.985 g, 1.19 mmol) in 15 mL of toluene was added a solution of $NaN(SiMe_3)_2{\cdot}THF$ (0.288 g, 1.13 mmol, 0.95 equiv) in 10 mL of toluene. The solution became yellow, and a fresh precipitate formed. The mixture was evaporated to dryness and the remaining solid extracted with toluene. The toluene solution was filtered through Celite and then allowed to slowly evaporate, producing yellow crystals of $[P_2N_2]TaMe_2F$. The crystals were crushed to a yellow powder and then thoroughly dried under high vacuum, producing **6** with 0.5 equiv of cocrystallized toluene that could not be removed (0.634 g, 70% yield). Solutions of **6** are mildly thermally sensitive. The same product was formed using lithium diisopropylamide as a base. ^1H NMR (C_6D_6, 340 K, 500 MHz): δ 0.28 and 0.33 (s, 24H total, SiCH_3), 1.27 (dt, $^2J_{PH}$ = 7.5 Hz, $^2J_{PF}$ = 6.2 Hz, 6H, TaCH_3), 1.55 and 1.55 (m, 8H, CH_2 ring), 7.10 and 7.15 (m, 6H total, *m*/*p*-*H*), 7.63 (m, 4H, *o*-*H*). $^{31}P\{^1H\}$ NMR (81.0 MHz, C_6D_6, 25 °C): δ 30.2 (s). ^1H NMR (500 MHz, C_7H_8, 240 K): δ 0.18, 0.22, 0.47, and 0.49 (s, 24H total, SiCH_3), 1.3, 1.3, 1.52, and 1.58 (m, 8H total, SiCH_2P), 1.30 (m, 6H, TaCH_3), 7.09 (m, 2H, *p*-*H*), 7.10 (m, 4H, *m*-*H*), 7.54 (m, 4H, *o*-*H*). $^{31}P\{^1H\}$ NMR (81.0 MHz, C_7D_8, 185 K): δ 26.5 (dd, $^2J_{PP}$ = 74.8 Hz, $^2H_{PF} \approx$ 70 Hz), 43.9 (d, $^2J_{PP}$ = 74.8 Hz). Anal. Calcd for $C_{26}H_{48}FN_2P_2$-

(39) Hagele, G.; Fuhler, R. DNMR-SIM, version 1.00, 1993.

$Si_4Ta \cdot 0.5C_7H_8$: C, 43.80; H, .48; N, 3.46. Found: C, 43.42; H, 6.69; N, 3.61.

$TaMe_2(CHSiMe_2NSiMe_2CH_2P(Ph)CH_2SiMe_2NSiMe_2CH_2PPh)$ (6). To a slurry of $\{[P_2N_2]TaMe_2\}^+B(C_6F_5)_4^-$ (0.713 g, 0.501 mmol) in 15 mL of toluene was added a solution of $NaN(SiMe_3)_2 \cdot THF$ (0.128 g, 0.501 mmol) in 10 mL of toluene. The color changed to yellow, and a light brown oil separated. The mixture was evaporated to dryness and the remaining solid extracted with toluene. The toluene solution was then evaporated to dryness, yielding **6** (0.348 g, 93% yield). The use of lithium diisopropylamide or $Me_3P{=}CH_2$ as a base also produced **6**. ^{1}H NMR (C_6D_6, 295 K, 500 MHz): δ −0.12, 0.08, 0.13, 0.27, 0.39, and 0.55 (s, 3H each, SiCH_3), 0.49 (d, $^4J_{HP}$ = 3.9, 3H, SiCH_3), 0.67 (d, $^4J_{HP}$ = 1.3, 3H, SiCH_3), 0.75 (ABX, $^2J_{HH}$ = 14.7, $^2J_{HP}$ = 7.0, 1H, SiC*H*HP), 1.12 (ABX, $^2J_{HH}$ = 14.7, $^2J_{HP}$ = 17.0, 1H, SiCH*H*P), 0.89 (ABX, $^2J_{HH}$ = 14.1, $^2J_{HP}$ = 7.3, 1H, SiC*H*HP), 1.23 (ABX, $^2J_{HH}$ = 14.1, $^2J_{HP}$ = 12.0, 1H, SiCH*H*P), 1.15 (ABX, $^2J_{HH}$ = 12.9, $^2J_{HP}$ = 8.8, 1H, SiC*H*HP), 1.37 (ABX, $^2J_{HH}$ = 12.9, $^2J_{HP}$ = 3.8, 1H, SiCH*H*P), 1.37 (d, $^3J_{HP}$ = 6.1, 6H, TaCH_3), 2.39 (dd, $^2J_{HP}$ = 2.8, $^3J_{HP}$ = 2.5, 1H, TaC*H*P), 7.08 (m, 1H, *p*-H), 7.12 (m, 2H, *m*-H), 7.14 (m, 1H, *p*-H), 7.31 (m, 2H, *m*-H), 7.48 (dd, $^3J_{HH}$ = 6.8, 2H, *o*-H), 7.79 (dd, $^3J_{HH}$ = 7.0, 2H, *o*-H). ^{31}P NMR (C_6D_6, 295 K): δ 17.9 (s, 1P, Ta*P*), −17.1 (s, 1P, TaCH*P*). ^{13}C (C_6D_6, 295 K): δ 1.9 (d, $^3J_{CP}$ = 3.8, SiCH$_3$), 2.7 (d, $^3J_{CP}$ = 20.0, SiCH$_3$), 3.9 (d, $^3J_{CP}$ = 4.3, SiCH$_3$), 4.0 (s, SiCH$_3$), 5.1 (s, SiCH$_3$), 5.5 (s, SiCH$_3$), 6.0 (s, SiCH$_3$), 6.4 (dd, J_{CP} = 7.1, J_{CP} = 9.1, SiCH$_3$), 16.8 (d, $^2J_{CP}$ = 2.9, SiCH$_2$P), 18.9 (d, $^2J_{CP}$ = 2.9, SiCH$_2$P), 20.7 (d, $^2J_{CP}$ = 29.1, SiCH$_2$P), 58.8 (dd, J_{CP} = 13.4, J_{CP} = 39.6, TaCHP), 66.8 (s, TaCH$_3$), 127.2 (s, PPh), 128.7 (d, J_{CP} = 4.8, PPh), 129.0 (d, J_{CP} = 8.6, PPh), 130.6 (d, J_{CP} = 1.9, PPh), 131.6 (d, J_{CP} = 17.2, PPh), 133.0 (d, J_{CP} = 10.4, PPh). Anal. Calcd for $C_{26}H_{47}N_2P_2Si_4Ta$: C, 42.04; H, 6.38; N, 3.77. Found: C, 42.41; H, 6.46; N, 3.61.

Effect of Photolysis Time on Conversion of 1 to 2. Using 42.55 mmol/L of ferrocene in C_6D_6 as an internal standard, a 32.6 mmol/L solution of **1** in C_6D_6 was prepared and sealed in a NMR tube. The tube was photolyzed for a measured period of time, and then the ^{1}H NMR spectrum was collected. The concentrations of **1** and **2** were obtained by integrating the ortho phenyl protons for the two species relative to the internal ferrocene standard. The photolysis was then continued, with spectra collected at 5, 11, 18, 24, 33, 44, 65, and 85 min. Photolysis time (min), yield of **2** (%), NMR-active Ta species remaining (%): 5, 27, 89; 11, 54, 89; 18, 58, 75; 24, 72, 59; 33, 61, 72; 44, 57, 69; 65, 53, 67; 85, 48, 64.

ESR of Products of Excessive Photolysis of 1. A solution of **1** in hexanes was sealed in an ESR tube equipped with a Teflon valve. The solution was photolyzed for 50 min, resulting in a dark green solution. EPR (hexanes): g = 1.93; $a(^{31}P)$ = 35 G, 2 P; $a(^{181}Ta)$ = 171 G, 1 Ta.

X-ray Crystallographic Analyses of 1 and 2. Crystallographic data appear in Table 1. The final unit-cell parameters were obtained by least-squares methods on the setting angles for 25 reflections with 2θ = 31.2−37.1° for **1** and 22 582 reflections with 2θ = 4.0−63.9° for **2**. The intensities of three standard reflections, measured every 200 reflections throughout the data collections, remained constant for **1**. The data were processed[40] and corrected for Lorentz and polarization effects and absorption. The structure of **1** was solved by heavy-atom Patterson methods and expanded Fourier techniques. There is a half-molecule of *n*-hexane per metal complex, located at a center of symmetry. The hexane molecule displays substantial thermal motion and is likely disordered. Several disorder models were tested, but none of them accounted for the electron density in this region as well as the simple, full-occupancy, anisotropic model including hydrogen atoms. A correction for secondary extinction was applied for **1** (coefficient [6.37(14)] × 10^{-7}). The structure of **2** was solved by direct methods and expanded Fourier techniques. The metal-bound methyl and methylene ligands were modeled as 1:1 disordered. For **2** the disordered carbon atoms were refined isotropically, while the remaining non-hydrogen atoms were refined anisotropically. In **1** all the non-hydrogen atoms were refined anisotropically. In both **1** and **2** hydrogen atoms were fixed in calculated positions with C−H = 0.98 Å. Those hydrogens associated with the disordered Ta−Me and Ta=CH_2 groups of **2** were not included. Neutral atom scattering factors for the non-hydrogen atoms were taken from ref 41. The absolute configuration of **2** was determined by Flack parameter refinement (0.047(5)). Atomic coordinates, anisotropic thermal parameters, all bond lengths and bond angles, torsion angles, intermolecular contacts, and least-squares planes are included as Supporting Information.

Acknowledgment. Funding for this research was provided by the NSERC of Canada in the form of a research grant to M.D.F. and a postgraduate scholarship to S.A.J.

Supporting Information Available: Full experimental details, tables of X-ray parameters, fractional coordinates and thermal parameters, bond lengths, bond angles, and torsion angles, and ORTEP diagrams for compounds **1** and **2** and variable-temperature NMR data analysis (Eyring plots) for fluxional processes observed in **1** and **2**. This material is available free of charge via the Internet at http://pubs.acs.org.

OM990249T

(40) teXsan: Crystal Structure Analysis Package; Molecular Structure Corp., The Woodlands, TX, 1995.

(41) (a) *International Tables for X-ray Crystallography*; Kynoch Press: Birmingham, U.K. (present distributor Kluwer Academic: Boston, MA), 1974; Vol. IV, pp 99−102. (b) *International Tables for Crystallography*; Kluwer Academic: Boston, MA, 1992; Vol. C, pp 200−206.